ON THE EFFICIENCY OF ANISOTROPIC DIFFUSION FILTERING SCHEMES

Cristian Cantón-Ferrer [*] **Bogdan Smolka** [**]
Marko Marcevski [***] **Zeina Torbey** [****]

[*] *Polytechnical University of Catalonia, Spain*
[**] *Silesian University of Technology, Poland*
[***] *Saint Cyril and Saint Metodius University, Macedonia*
[****] *Damascus University, Syria*

Abstract: The aim of the work presented in this paper is to investigate experimentally the behavior of different types of anisotropic diffusion schemes. The efficiency of the filters based on the anisotropic diffusion is determined to large extent by the properties of the *conductance function* in the PDE equation, which describes the diffusion process. Changing the shape of the conductivity function, we can tune the anisotropic diffusion filter to the image noise intensity and its statistical properties, in order to achieve optimal results of the image smoothing. This paper analyzes the behavior of the classical functions introduced by Perona and Malik together with the Tukey's biweight and Huber's minmax function introduced by Black et al. and compares the different filtering schemes with the standard approaches used for the reduction of Gaussian noise in digital images.

Keywords: Nonlinear filters; Image enhancement; Noise reduction; Anisotropic diffusion.

1. INTRODUCTION

Filtering is the first and one of the most important image processing steps in most of the image analysis and computer vision applications. Its goal is the removal of unprofitable information that may corrupt any following processing.

The acquisition or transmission of digital images through sensors or communication channels is often inferred by mixed impulsive and Gaussian noise. In many applications it is indispensable to remove the corrupted pixels to facilitate subsequent image processing operations such as edge detection, image segmentation and pattern recognition.

Different filtering schemes based on nonlinear diffusion, developed for image enhancement have been achieving more and more importance in the last decade. One of the main goals of these algorithms is to restore the image corrupted with noise, while preserving the edges, corners and other important image features.

2. ANISOTROPIC DIFFUSION

Let $I(x, y) \in [0, 1]$ represents an image with real-valued intensities at positions (x, y) in the image domain Ω. The original image will be modifyied using a partial derivative equation (PDE) and let $I^t(x, y)$ be the image at time (iteration) t.

The main concept of *Anisotropic Diffusion* is based on the modification of the isotropic diffusion equation [1], to inhibit the smoothing of image edges. This modification is done by introducing a function $c(x, y, t)$ that encourages intra-region smoothing over inter-region smoothing. Perona and Malik [2] proposed a nonlinear anisotropic dif-

fusion equation, where the conduction coefficient $c(x,y,t)$ is dependent on the image structure [2 - 7] :

$$\frac{\partial I(x,y,t)}{\partial t} = \nabla \cdot [c(x,y,t) \quad \nabla I(x,y,t)] \ ,$$
$$c(x,y,t) = f(\|\nabla I(x,y,t)\|) \ , \qquad (1)$$

where $\|\nabla I(x,y,t)\|$ is the gradient magnitude, and $c(\|\nabla I(x,y,t)\|)$ is the nonlinear *conduction function*, that determines the behavior of the diffusion process.

2.1 Discrete Anisotropic Diffusion

Anisotropic diffusion equation may be implemented in discrete terms as:

$$I_r^{(t+1)} = I_r^{(t)} + \frac{\lambda}{|\mathcal{N}_r|} \sum_{p \in \mathcal{N}_r} c\left(\|\nabla I_{r,p}^{(t)}\|\right) \nabla I_{r,p}^{(t)} \ , (2)$$

where I_r^t is a discretely sampled image at the spatial position r. The constant $\lambda \in \mathbb{R}^+$ is a scalar parameter that determines the rate of the diffusion process, $\mathcal{N}_r$ denotes the spatial neighborhood of the pixel located at the position r and $|\mathcal{N}_r|$ is the number of neighbors of the center pixel.

The gradients can be linearly approximated in a chosen direction p as:

$$\nabla I_{r,p}^{(t)} = I_r^{(t)} - I_p^{(t)}, \qquad p \in \mathcal{N}_r \ . \qquad (3)$$

3. CONDUCTION FUNCTIONS

The function that impedes the smoothing across the edges in the anisotropic diffusion scheme, is the diffusion coefficient. The conduction function $c(\|\nabla I(x,y,t)\|)$, denoted as $c(s)$ is space varying (depending on the gradient magnitude s at a determined position) and is chosen to be large in homogeneous regions to encourage image smoothing and small at edges to preserve image structures. This function should satisfy four properties:

(1) $c(0) = M$ where $0 < M < \infty$,
(2) $c(s) = 0$, when $s \to \infty$,
(3) $c(s) \geq 0$
(4) $s \cdot c(s)$ is a strictly decreasing function.

Property (1) ensures isotropic smoothing in regions of similar intensity, while the property (2) ensures the edge preservation. The last property is given in order to avoid numerical instability. The stability of the nonlinear PDE equation was the particular concern of extensive research [4 - 6]. While most of the coefficients discussed here obey the first three properties, not all formulations obey the last one.

If the nonnegativity condition is not satisfyied a backward diffusion proces will be performed [2,7]. The conduction functions used in the simulations described in this paper accomplish the first three properties, the last one is not satisfied, which can lead to the backward diffusion and ill-posedness of the PDE.

Perona and Malik originally suggested two ill-posed choices of $c(s)$, (Fig. 1):

$$c_1(s) = \frac{1}{1 + \left(\frac{s}{K}\right)^2}, \quad c_2(s) = \exp\left\{-\left(\frac{s}{K}\right)^2\right\} (4)$$

The constant K can be made adaptive, using the "noise estimator" described in [8], where a histogram of the absolute values of the gradients throughout the image is computed and K is equal to the 90% value of its integral.

Different functions that satisfy the first three properties can be chosen. In [9], robust statistic norms were chosen to define the conduction functions. The authors proposed there the *Tukey's biweight function*, (Fig. 1) :

$$c_3(s) = \begin{cases} \frac{1}{2}\left[1 - \left(\frac{s}{S}\right)^2\right]^2 & , \ s \leq S, \\ 0 & , \text{otherwise.} \end{cases} \qquad (5)$$

Another function extracted from the robust statistics literature is the *Huber's minimax norm* [10]:

$$c_4(s) = \begin{cases} 1/S & , \ |s| \leq S, \\ \text{sign}(s)/s & , \ |s| > S. \end{cases} \qquad (6)$$

According to the authors of [10], these conductivity functions should lead to a more robust anisotropic diffusion filters, which better cope with the smoothing of noisy images. The aim of this work is to evaluate the performance of those two functions as compared with the functions introduced by Perona and Malik [2].

4. RESULTS OF THE COMPARISON

In order to compare the efficiency of the anisotropic diffusion filtering schemes based on different conductivity functions, we contaminated the LENA and PEPPERS standard gray scale images with zero-mean, additive Gaussian noise of $\sigma = 10, 20$ and 30 respectively. For each conductivity function we searched for the optimal combination of λ and the K or S constant parameters. For each combination of λ and the second parameter, we iterated the diffusion process untill the maximum PSNR value was achieved. From all the combinations of filters' parameters we found the best possible value for each conductivity function and treated this value as an indicator of the filter's performance.

The efficiency of the four filtering schemes is shown in Figs. 2 and 4. Figures 6, 7 show the evolution of PSNR with the iteration number for

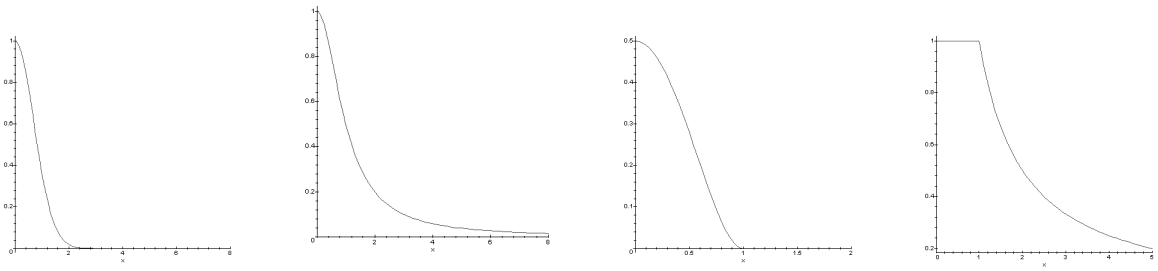

(a) (b) (c) (d)

Fig. 1. Plots of the conductivity functions: (a) Gaussian - c_1; (b) $1/(1+(s/K)^2)$ - c_2; (c) Tukey's biweight - c_3; (d) Huber's minmax - c_4.

the optimal parameter settings. We observe, that for all four evaluated conductivity functions, only one local maximum can be found and further iterations decrease slowly the image quality introducing too much smoothing.

Figures 3 and 5 show the results of noise attenuation obtained using some of the standard filters. For the comparison we used the α trimmed filters, mean average and the median.

5. CONCLUSIONS

Our simulations revealed that for the the images distorted by Gaussian noise of $\sigma = 10, 20$ and 30, the c_1 function yielded slightly better results than the Gaussian c_2. Surprisingly, the robust conductivity functions c_3 and c_4 were not at all significantly superior to the functions c_1 and c_2 originally proposed by Perona and Malik (the $c-3$ yielded slightly better results than c_2. There were no significant differences in the PSNR values obtained using the robust functions c_3 and c_4. The filtering scheme based on the Huber minmax gave the poorest results.

The efficiency of the anisotropic diffusion decreases with the intensity of the Gaussian noise and for $\sigma = 30$ this filtering scheme is significantly worse than the simple α-trimmed mean, which by the way performed better than the 3×3 median. This inability of the anisotropic diffusion filters to suppress strong Gaussian noise can be derived from the fact that strong impulses introduced by the noise process are perceived by the filters as edges and are not eliminated, which leads to a poor filter performance. We expected that the conductivity functions based on the robust statistics would perform significantly better for strongly degraded images, than the simple functions c_1 and c_2. Our extensive simulations revealed however, that the robust conductivity functions do not improve the filter performance. In fact their performance was even slightly worse than when using the functions proposed by Perona and Malik.

The performed study shows, that for the Gaussian additive noise of low intensity, the anisotropic diffusion based on the c_1 conduction coefficient is a very good choice. The *robust statistics* described in [9] failed to increase the efficiency of the anisotropic diffusion based noise filtering.

REFERENCES

[1] A. Witkin, Scale-space filtering, Int. Joint Conf. Artif. Intell., 1983, 1019–1021

[2] P. Perona, J. Malik, Scale-space and edge detection using anisotropic diffusion, IEEE Trans. Pattern Anal. Machine Intell., 1990, PAMI-12. No. 7, 629–639

[3] L. Alvarez, F.Guichard, P.L. Lions, J.M. Morel, Image selective smoothing and edge detection by nonlinear diffusion, SIAM J. Numer. Anal., 1993, 29, 845–866

[4] F. Catté, F. Dibos, G. Koepfler, Image selective smoothing and edge detection by nonlinear diffusion, SIAM J. Numer. Anal., 1992, 29, 182–193

[5] J. Weickert, Anisotropic Diffusion in Image Processing, G. G. Teubner, 1998, Stuttgart

[6] Y. You, W. Xu, M. Kaveh, A. Tannenbaum, Behavioral analysis of anisotropic diffusion in image processing, IEEE Trans. Image Processing, 1996, 5, 1539–1553

[7] G. Gilboa, Y. Zeevi, N. Sochen, Resolution enhacement by forward-and-backward nonlinear diffusion processes, Nonlinear Signal and Image Processing, Baltimore, Maryland, June 2001

[8] J. Canny, A computational approach to edge detection, IEEE Trans. Pattern Anal. Machine Intell., 1986, PAMI-8, 679–698

[9] M. J. Black, G. Sapiro, D. H. Marimont, M. J. Black, D. Heeger, Robust anisotropic diffusion, IEEE Trans. Image Processing, 1998, Vol. 7, No. 3, 421–432

[10] P. J. Huber, Robust Statistics, New York, Wiley, 1981

6. ACKNOWLEDGEMENTS

This work was performed at the Computer Vision Laboratory of the Silesian University of Technology in Gliwice, Poland. Cristian Cantón-Ferrer, Marko Marcevski and Zeina Torbey were supported by the Silesian University of Technology, Department of Automatic Control and the IAESTE Student Exchange Program. Bogdan Smolka was partially supported by KBN Grants: 7 T11A 010 21, PBZ-KBN-040/P04/08, NATO Collaborative Linkage Grant LST.CLG.977845,

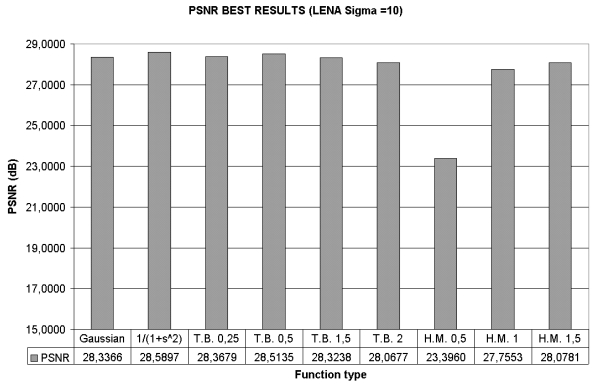

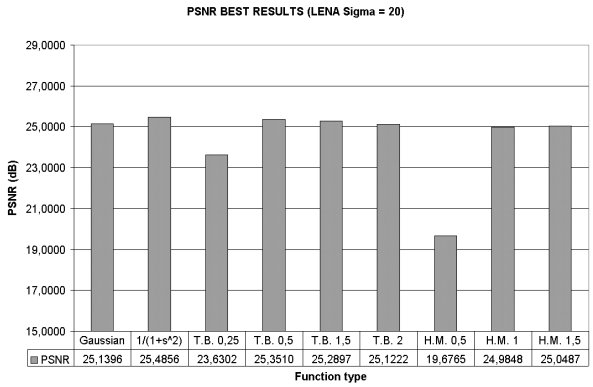

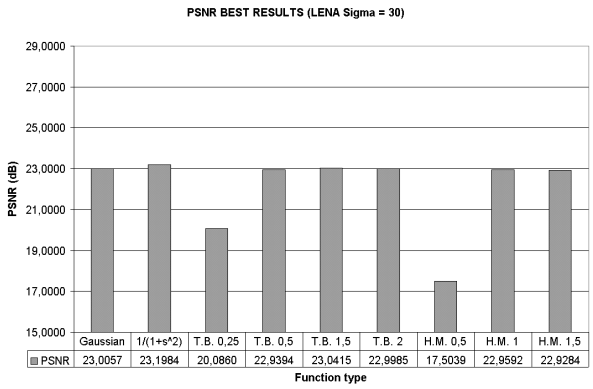

Fig. 2. The efficiency of the anisotropic diffusion filters in terms of PSNR. For the evaluation purposes 15 iterations were computed for the gray scale LENA image distorted by zero-mean additive Gaussian noise using different conductivity functions (c_1, c_2, c_3 and c_4) described in this paper and λ values ranging from 1/8 to 1/100. For each conductivity function the optimal settings of the parameters were found and the best possible PSNR results were selected as indicators of the specific filter performance.

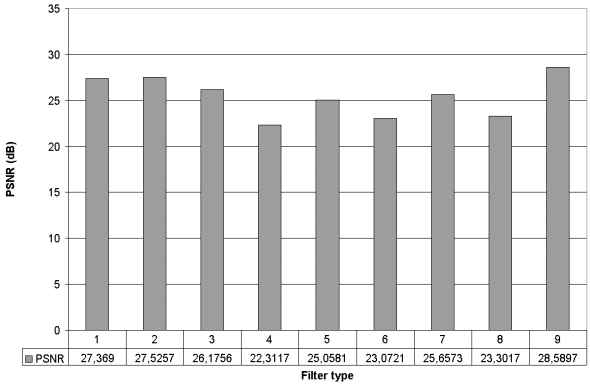

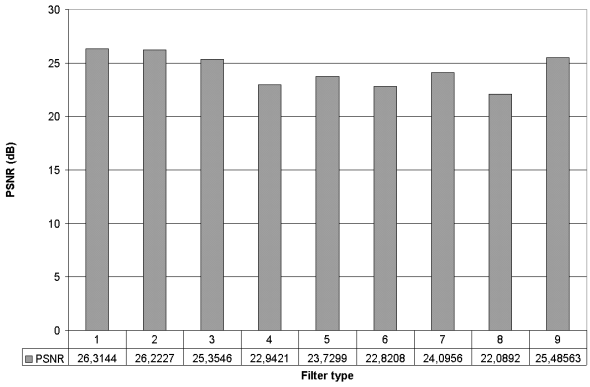

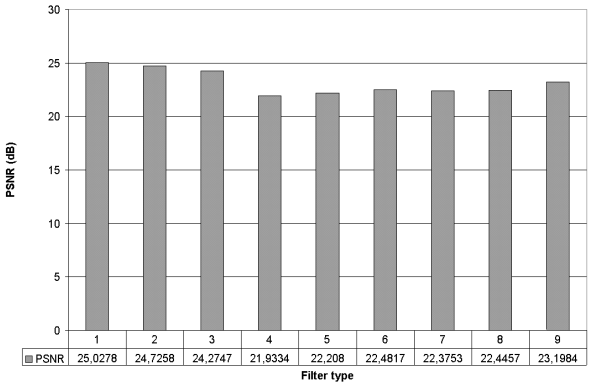

Fig. 3. PSNR results obtained with other commonly used filters using the same distorted LENA images: (1) α-trimmed (2 excluded pixels), (2) α-trimmed (4 excluded pixels), (3) moving average (3x3), (4) moving average (5x5) (5) median filter (3x3, 2 iterations), (6) median filter (5x5, 2 iterations) (7) median filter (3x3), (8) Median filter (5x5), (9) Anisotropic diffusion with c_1.

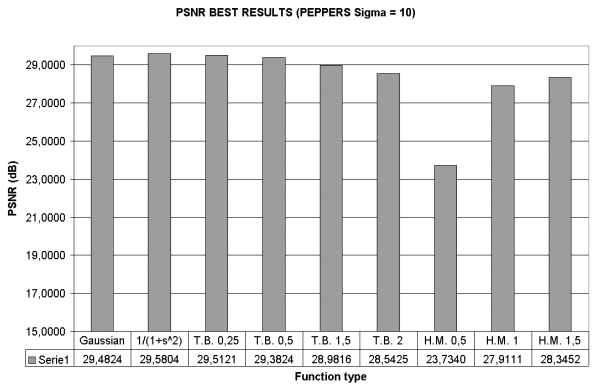

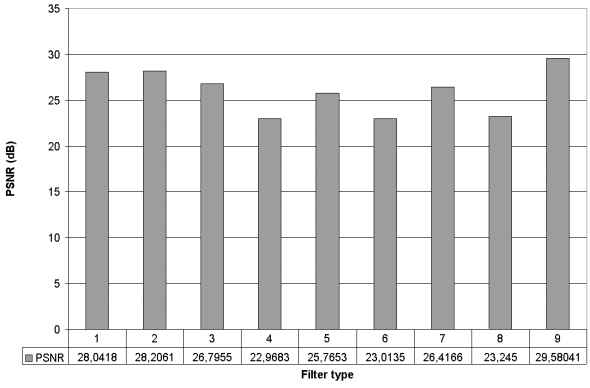

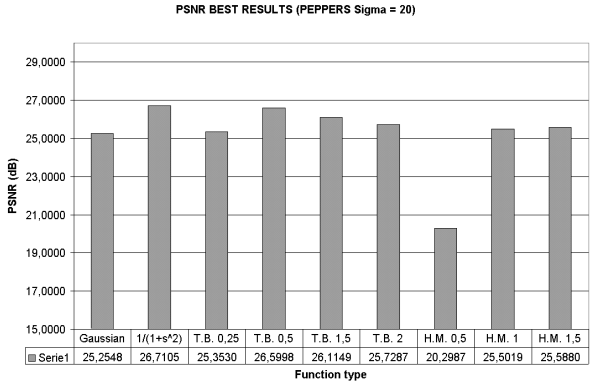

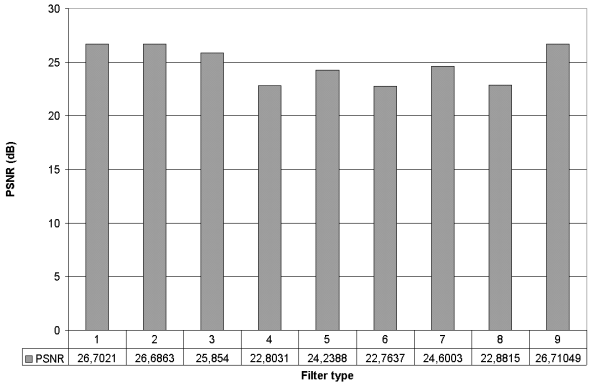

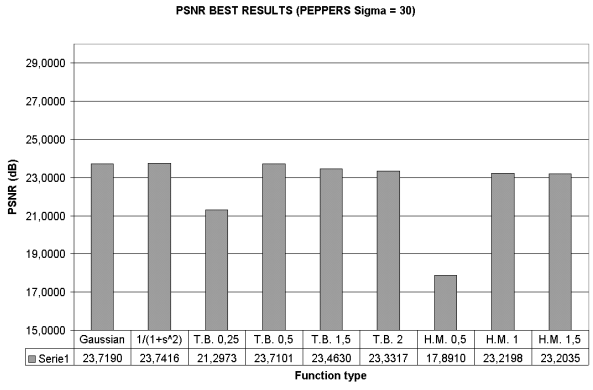

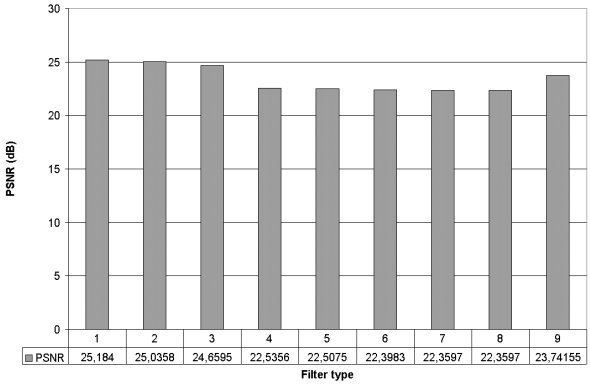

Fig. 4. The efficiency of the anisotropic diffusion filters in terms of PSNR. For the evaluation purposes 15 iterations were computed for the gray scale PEPPERS image distorted by zero-mean additive Gaussian noise using different conductivity functions (c_1, c_2, c_3 and c_4) described in this paper and λ values ranging from 1/8 to 1/100. For each conductivity function the optimal settings of the parameters were found and the best possible PSNR results were selected as indicators of the specific filter performance.

Fig. 5. PSNR results obtained with other commonly used filters using the same distorted PEPPERS images: (1) α-trimmed (2 excluded pixels), (2) α-trimmed (4 excluded pixels), (3) moving average (3x3), (4) moving average (5x5) (5) median filter (3x3, 2 iterations), (6) median filter (5x5, 2 iterations) (7) median filter (3x3), (8) Median filter (5x5), (9) Anisotropic diffusion with c_1.

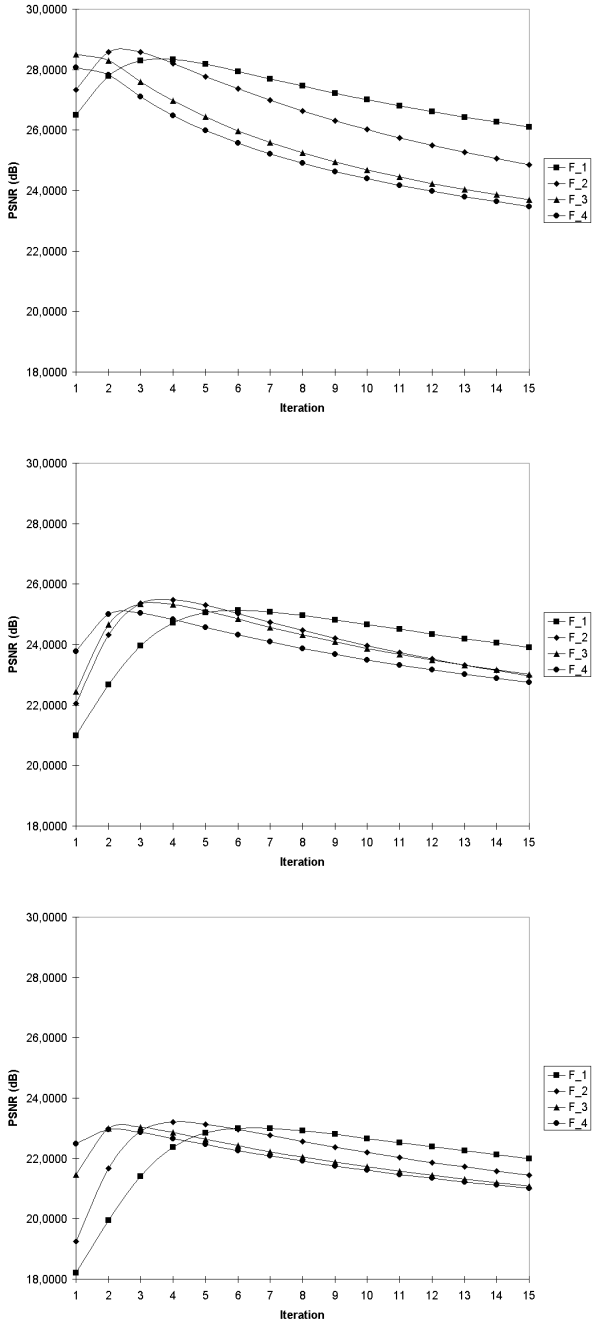

Fig. 6. The dependence of the PSNR on the iteration number using different conductivity functions, (LENA).

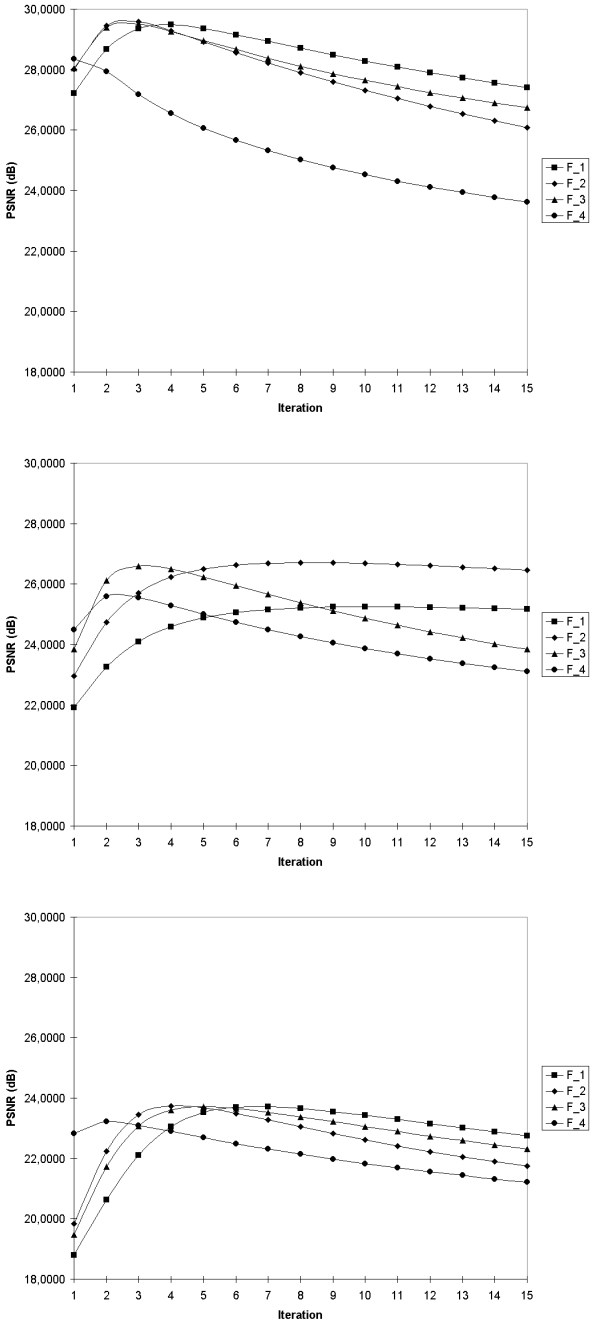

Fig. 7. The dependence of the PSNR on the iteration number using different conductivity functions, PEPPERS).